FUDMA Journal of Sciences (FJS)
ISSN online: 2616-1370
ISSN print: 2645 - 2944
Vol. 9 No. 10, October, 2025, pp 296 – 311
DOI: https://doi.org/10.33003/fjs-2025-0910-3837

NUMERICAL SIMULATION AND ANALYSIS OF A CAPUTO FRACTIONAL-ORDER SEIR MODEL FOR COVID-19 PREVALENCE USING THE HERMITE POLYNOMIAL COLLOCATION AND LAPLACE-ADOMIAN DECOMPOSITION METHODS

[1]Morufu Oyedunsi Olayiwola, [1]Ajimot Folasade Adebisi, *[2]Bosede Abubakar and [1]Akeem Olarewaju Yunus

[1]Department of Mathematical Science, Osun State University, Osogbo, Nigeria.
[2]Department of Mathematics, University of Ilesa, Ilesa, Nigeria.

*Corresponding author's email: bosede_abubakre@unilesa.edu.ng

ABSTRACT

COVID-19 poses major public health challenges due to its high transmissibility. This study presents a novel numerical framework based on a fractional-order SEIR model to explore serotonin transfer and evaluate control strategies for emerging SARS-CoV-2 variants. By including the exposed compartment, the extended SEIR model offers improved insight into variant transmission dynamics. Two advanced numerical techniques are compared: the Hermite Collocation Method (HCM) and the Laplace-Adomian Decomposition Method (LADM). Due to the model's inherent nonlinearity, finding exact solutions is difficult. To overcome this, the model is transformed into a nonlinear algebraic system using Hermite polynomial collocation with Caputo fractional derivatives. Expansion coefficients representing the approximate solution are computed with Maple software, enabling precise analysis of disease dynamics. The fractional derivative framework captures memory effects that influence transmission, particularly under changing viral conditions. Simulations reveal that both methods effectively reduce transmission and hospitalizations, but HCM outperforms LADM in accuracy and convergence speed. The results demonstrate the strength of fractional-order modeling in describing real-world epidemic patterns, especially with evolving COVID-19 variants. HCM's high reliability positions it as a valuable predictive tool for health authorities. Its precision allows for early detection of outbreaks and supports the formulation of responsive public health strategies. This study emphasizes the importance of advanced mathematical modeling in managing infectious diseases and recommends HCM as a reliable method for anticipating variant behavior. Policymakers can apply this approach to develop timely, adaptive interventions for future COVID-19 variants and similar pandemics.

Keywords: Hermite Polynomials, Collocation Methods, SARS-CoV-2 Variants, Laplace-Adomian Decomposition Method, Simulations Analysis

INTRODUCTION

Here's the combined introduction with corrected reference formatting: The SARS-CoV-2 pandemic significantly transformed global health systems, causing over 7 million deaths worldwide and highlighting the necessity for advanced modeling and control measures (Apostolopoulos *et al.*, 2024; Gheisari, 2024). Mathematical modeling played a critical role in understanding COVID-19 transmission patterns and evaluating interventions such as vaccination and social distancing (Yadav, 2020; Yunus & Olayiwola, 2024a). Previous studies demonstrated that COVID-19 spread in Southeast Asia could be effectively modeled using SEIR with actual data, showing R_0 dropped from high initial values to ~3 after lockdown, projecting maximum 2500 active cases with decline by June 2020 (Jacob *et al.* 2022). While classical integer-order models often fail to capture the long memories and nonlinearities of actual epidemics, fractional models based on Caputo or Caputo-Fabrizio derivatives have shown superior flexibility in capturing memory dynamics and have been successfully applied to various infectious diseases (Yunus *et al.*, 2023; Asimiyu *et al.*, 2025). Among numerical solution techniques, the Hermite Collocation Method (HCM) has demonstrated superior accuracy over traditional methods like LADM in solving nonlinear epidemiological equations, proving that timely public health interventions are critical for effective disease control (Olayiwola *et al.* 2025). This paper constructs a memory-based fractional-order SEIR model for COVID-19 transmission dynamics, comparing HCM and LADM solutions to provide a framework for accurate epidemic modeling and real-time policy intervention planning.

MATERIALS AND METHODS

Preliminaries

Basic ideas of fractional calculus that are pertinent to the study

Definition 1

$\vartheta(z)$, forz $> 0 \exists \aleph_\gamma, \gamma \in R, if \kappa > \gamma: \vartheta(z) = z^k \vartheta_1(z)$.
in which $\vartheta_1(z) \in \gamma(0,\infty)$, It is claimed that $\vartheta(z)$ exists in space $\gamma_v^\alpha, iff \vartheta^{(\alpha)} \in \gamma_v, \varpi \in I$..

Definition 2

Caputo fractional derivative is expressed as
$;U^\eta \vartheta(z) = \frac{1}{\Gamma(\eta-\lambda)} \int_0^x (z-t)^{\eta-\gamma-1} \vartheta^{(z)}(t)dt, \eta - 1 < \gamma \leq \eta, \eta \in N$.

Definitions 3

The Laplace transform of $\vartheta(t)$ is the function $\vartheta(s): \vartheta(s) = \int_0^\infty e^{-st} \vartheta(t)\, dt$
$\vartheta of order \eta \therefore taking Laplace of [\eta^\eta(t)] = v^\eta L[\eta(t)] - v^{\eta-1}\eta(0) - v^{\eta-2}\vartheta'(0) - v^{\eta-3}\vartheta''(0)$
$L^{-1}\frac{\vartheta(v)}{v} = \int_0^t \vartheta(t)dt$ (Inverse Laplace transforms of $\frac{\vartheta(v)}{v}$)
$f(t) = t^\lambda$is,$L(t^\lambda) = \frac{\Gamma(\partial+1)}{v^{\lambda+1}}$,
then
$L^{-1}\left(\frac{1}{v^{\lambda+1}}\right) = \frac{t^\lambda}{\Gamma(\lambda+1)}$ $L^{-1}\left(\frac{1}{v^{\partial+1}}\right) = \frac{t^\lambda}{\Gamma(\partial+1)}$

Definition 4
$A_0, A_{1,\dots,}A_n$, represents the Adomian polynomialencompasses the breakdown $y(t)$ represented as. $y(t) = y_0 + y_1 + y_2 + \cdots y_n$is presented as:

$$M_z = \frac{1}{z}\frac{d^z}{d\partial^z}\left[A(t)\sum_{j=0}^{n} z_j\partial^j\right]_{\lambda=0}$$

Step Flow of Thegeneral Hermite Polynomial
$H_n(x)$, is given by the Rodrigues formula:

$$H_n(x) = \frac{(-1)^n d^n}{w(x)dx^n}\{w(x) * g(x)\}$$

Where:$w(x) =$ is the weight function, $g(x) =$ is the scaling function
$n$is the order of the polynomial., We'll assume:$w(x) = e^{-x^2}$, the classical weight function
$g(x) = 1$, to simplify the general form'
Step 1:
for $n = 0$
Substitute $n = 0$

$$H_0(x) = \frac{(-1)^0}{e^{-x^2}} \times \frac{d^0}{dx^0}(e^{-x^2} \times 1^0)$$

$$H_0(x) = \frac{1}{e^{-x^2}} \times e^{-x^2} = 1$$

So, the 0th Hermite polynomial is: $H_0(x) = 1$
Step 2:
for $n = 1$, Substitute n=1 into the formula: $H_1(x) = \frac{(-1)^1}{e^{-x^2}} \times \frac{d}{dx}[e^{-x^2} \times 1^1]$,
Differentiatee^{-x^2}, $\frac{d}{dx}(e^{-x^2}) = -2xe^{-x^2}$
Substitute back: $H_1(x) = \frac{-1}{e^{-x^2}} \times (-2xe^{-x^2})$
Simplify:$H_1(x) = 2x$
So, the 1st Hermite polynomial is: $H_1(x) = 2x$
Step 3:
For n=2 Substitute n=2into the formula:$\boldsymbol{H_2(x)} = \frac{(-1)^2}{e^{-x^2}} \times \frac{d^2}{dx^2}(e^{-x^2} \times 1^2)$

First derivative:$\frac{d}{dx}(e^{-x^2}) = -2xe^{-x^2}$Second derivative:$\frac{d^2}{dx^2}(e^{-x^2}) = \frac{d}{dx}(-2xe^{-x^2}) = -2e^{-x^2} + 4x^2e^{-x^2}$
Substitute back:$H_2(x) = \frac{1}{e^{-x^2}} \times (-2x^{-x^2} + 4x^2e^{-x^2})$,
Simplify:$H_2(x) = -2 + 4x^2$
So, the 2nd Hermite polynomial is:$H_2(x) = 4x^2 - 2$
The first three Hermite polynomials are: By following the same process, higher-order Hermite polynomials can be computed systematically.
Which can be presented as function below

$$H_0 = 1$$
$$h_1 = 2x$$
$$H_2 = 4x^2 - 2$$
$$H_3 = 8x^3 - 12x$$
$$H_4 = 16x^4 - 48x^2 + 12$$
$$H_5 = 32x^5 - 160x^3 + 120x$$
$$H_6 = 64x^6 - 480x^4 + 720x^2 - 12$$
$$H_7 = 128x^7 - 1344x^5 + 3360x^3 - 1680x$$
$$H_8 = 256x^8 - 3584x^6 + 13440x^4 - 1344x^2 + 1680$$

.
.
.

$\cdot H_n(x) = \sum_{n=0}^{\frac{n}{2}} \frac{(-1)n!(2x)n - 2m}{m!(n-2m)!} H_n(x)$ and its derivative at $x = 0$f$H_n(x) =$
$\sum_{n=0}^{\frac{n}{2}}(-1)^m \frac{n!}{m!(n-2m)!}(2x)^{n-2m}{}_{e}\left(\frac{n}{2}\right)=$

$$\begin{cases} \frac{n}{2} \ if \ nis \ even \\ \frac{n-1}{2} if \ n \ is \ odd \end{cases} H_n(x) =$$

$\sum_{m=0}^{n} \frac{(-1)^m(2n)!(2x)^{2n-2m}}{m!(2n-2m)!} H_{2n}(0) = \frac{(-1)^n(2n)!}{n!} = \frac{(-1)^n(1)_{2n}}{n!} =$
$[1.(2n!) = (1)2n] =$
$(-1)^n 2^{2n} \left(\frac{1}{2}\right)_n \left(\frac{2}{2}\right)_n = \frac{(-1)^n 2^{2n}\left(\frac{1}{2}\right)_n (1)n}{n!} \frac{(-1)^n 2^{2n}\left(\frac{1}{2}\right)_{nn!}}{n!} H_2 n(0) =$
$(-1)^n 2^{2n}\left(\frac{1}{2}\right)_n$

Step Flow of the LADM
${}_t^cU^\eta g_k(t) = J_k(g_1, g_2, g_3, \cdots g_k) + N_k(g_1, g_2, g_3, \cdots g_k)$ fractional-order differential equation.
Assuming
$z_c^{i_k}(0) = b_i^c$, for $c = 1,2,3\dots m$, and$n_{k-1} \le \alpha \le n_k$.
${}_t^cU^\eta f_k(t)$ Represents the Caputo-derivative of a few unknown functions$f(t)$,L_k and $N_k$are linear and nonlinear operators.
Utilize the LADM for the solution of the system. :

$$L[\ {}_t^cU^\alpha g_h(t)] = L[J_h(g_1, g_2, g_3, \cdots g_k) + N_k(g_1, g_2, g_3, \cdots g_h)]$$

$$v^\eta L[g_h(t)] - \sum_{i=0}^{m-1} v^{\eta_k - i - 1}c_i^h = L[J_h(g_1, g_2, g_3, \cdots g_h) + N_h(g_1, g_2, g_3, \cdots g_h)]$$

$$L\left[\sum_{j=0}^{\infty} g_{kj}(t)\right] = \frac{1}{v^{\eta_k}}\sum_{i=0}^{m-1} v^{\alpha_k - i - 1}c_i^k + \frac{1}{v^{\eta_k}} L\left[L_k\left(\sum_{j=0}^{\infty} g_{1j}(t), \dots, \sum_{j=0}^{\infty} g_{mj}(t)\right)\right] + \frac{1}{v^{\eta_k}} L\left[\sum_{j=0}^{\infty} A_{kj}(t)\right]$$

Then, we make use of the Laplace transforms linearity property to create a recursive formula that looks like this:

$$L[g_h] = \frac{1}{v^{\alpha_k}}\sum_{j=0}^{m-1} v^{\alpha_k - i - 1}c_i^h, h = 1,2,3\dots.z$$

$$L[g_{h(j+1)}(t)] = \frac{1}{v^{\alpha_k}} L[L_h(\sum_{j=0}^{\infty} g_h(t), \dots, \sum_{j=0}^{\infty} g_{mj}(t))] + \frac{1}{S^{\alpha_k}} L(\sum_{j=0}^{\infty} A_{kj}(t))$$

$$g_{h(j+1)}(t) = L^{-1}\left(\frac{1}{v^{\alpha_k}} L[L_h(\sum_{j=0}^{\infty} g_{1j}(t), \dots, \sum_{j=0}^{\infty} g_{mj}(t))] + \frac{1}{v^{\alpha_k}} L[\sum_{j=0}^{\infty} A_{kh}(t)]\right)$$

Methodology
Classical Order Model Formulation Descriptions Variant
This section deploys an SEIR-based mathematical model that builds on Aydin, S. (2018) SIR framework by including an Exposed sub compartment to portray viral variant transmission dynamics. The model tracks SARS-CoV-2 variant transmission dynamics by identifying important factors between exposed to infected stages and recovery times

with transmission rate parameters. People within the population fit into four groups consisting of susceptible, exposed, infected and recovered according to this framework that shows their active participation in spreading disease.

$$\frac{dS(t)}{dt} = -\beta S(t)I(t)$$
$$\frac{dI(t)}{dt} = \beta S(t)I(t) - \gamma I(t)$$
$$\frac{dR(t)}{dt} = \gamma I(t)$$

The Modified Model

$$\frac{dS(t)}{dt} = -\beta S(t)I(t)$$
$$\frac{dE(t)}{dt} = \beta S(t)I(t) - \alpha E(t)$$
$$\frac{dI(t)}{dt} = \alpha E(t) - \gamma I(t)$$
$$\frac{dR(t)}{dt} = \gamma I(t) \qquad (2)$$

The set of equations now includes the Caputo fractional order derivative, which improves the mathematical model. This improvement allows the memory effect to be studied using fractional-order derivatives. The system of ordinary differential equations has been modified as a result, as explained below

$$^{c}\chi S(t) = -\beta S(t)I(t)$$
$$^{c}\chi E(t) = \beta S(t)I(t) - \alpha E(t)$$
$$^{c}\chi I(t) = \alpha E(t) - \gamma I(t)$$
$$^{c}\chi R(t) = \gamma I(t) \qquad (3)$$

Where: $S(t)$ Represents the susceptible population, $E(t)$ Represents the exposed population,
$I(t)$ Represents the infectious population, $R(t)$ Represents the recovered population,
β Transmission rate, α Rate of progression from exposed to infected, γ Recovery rate.

Application of Hermite Collocation Method (HCM) to the Model

By applying HCM, the functions $S(t), E(t), I(t), R(t)$. are expressed as truncated Hermite polynomial series: Expand the variables using Hermite Polynomial assume approximate solution for equation (3) as finite series of Hermite Polynomial:

$$\left.\begin{aligned} S(t) &= \textstyle\sum_{n=0}^{N} c_{1,n}H_n(t) \\ E(t) &= \textstyle\sum_{n=0}^{N} c_{2,n}H_n(t) \\ I(t) &= \textstyle\sum_{n=0}^{N} c_{3,n}H_n(t) \\ R(t) &= \textstyle\sum_{n=0}^{N} c_{4,n}H_n(t) \end{aligned}\right\} \qquad (4)$$

Where,
N: is the degree of the Hermite expansion and c_1, c_2, c_3, c_4 are coefficients to be determined
Now, involve sum of Hermite Polynomial and their Derivatives by substituting Hermite expansion of (4) into (3), which gives;

$$\frac{dS}{dt} = -\beta S(t)I(t)$$
$$\frac{d}{dt}\left(\sum_{n=0}^{N} a_nH_n(t) - \beta\left(\sum_{n=0}^{N} a_nH_n(t)\right)\left(\sum_{m=0}^{N} c_mH_m(t)\right)\right)$$
$$\frac{dE}{dt} = -\beta S(t)I(t) - \alpha E(t)$$
$$\frac{d}{dt}\left(\sum_{n=0}^{N} b_nH_n(t) - \beta\left(\sum_{n=0}^{N} a_nH_n(t)\right)\left(\sum_{m=0}^{N} c_mH_m(t)\right)\right) - \alpha\left(\sum_{=0}^{N} b_pH_p(t)\right)$$
$$\frac{dI}{dt} = \alpha E(t) - \gamma I(t)$$
$$\frac{d}{dt}\left(\sum_{n=0}^{N} C_MH_{n_M}(t) = \alpha\left(\sum_{n=0}^{N} B_PH_P(t)\right) - \gamma\left(\sum_{m=0}^{N} c_mH_m(t)\right)\right)$$
$$\frac{dR}{dt} = \gamma I(t)$$

$$\frac{dR}{dt} = \gamma\left(\textstyle\sum_{m=0}^{N} C_mH_m(t)\right) \qquad (5)$$

The Derivatives of (5) are $\frac{d}{dt}H_n(t) = 2nH_{n-1}(t)$ (property of Hermite polynomial) $\frac{d}{dt}\left(\sum_{n=0}^{N} a_nH_n(t)\right) = \sum_{n=0}^{N} a_n \times 2nH_{n-1}(t)$

$$= \sum_{n=1}^{N} 2na_nH_{n-1}(t)$$
$$-\beta S(t)I(t) = \left(\sum_{n=0}^{N} a_nH_n(t)\right)\left(\sum_{m=0}^{N} c_mH_m(t)\right) - \beta\sum_{k=0}^{2N} a_kc_kH_k(t)$$
$$\sum_{n=1}^{N} 2na_nH_{n-1}(t) = -\beta\sum_{k=0}^{2N} a_km_kH_k(t)$$
$$\frac{d}{dt}\left(\textstyle\sum_{n=0}^{N} b_pH_P(t)\right) = \sum_{n=0}^{N} b_p \times 2_pH_p - \sum_{n=1}^{N} 2_pb_pH_{p-1}(t)$$
$$\beta SI(t) = \sum_{k=0}^{2N} a_nc_mH_{n+m}(t) \Rightarrow \beta\sum_{n=0}^{N}\sum_{m=0}^{N} a_nc_mH_{n+m}(t) - \alpha\sum_{p=0}^{N} b_pH_p(t)$$
$$\frac{d}{dt}\left(\sum_{n=0}^{N} c_mH_m(t)\right) - \alpha\sum_{n=0}^{N} b_pH_p(t) - \gamma\sum_{m=1}^{N} c_mH_m(t)$$
$$\frac{d}{dt}\left(\sum_{m=0}^{N} c_mH_m(t)\right) = \sum_{m=0}^{N} c_m.2mH_{m-1}(t) \Rightarrow \sum_{m=1}^{N} 2mc_mH_{m-1}(t)$$
$$\alpha E(t) = \alpha\sum_{m=0}^{N} b_pH_p$$
$$\gamma I(t) = -\gamma\sum_{m=0}^{N} c_m\,H_m(t)$$
$$\Rightarrow \alpha\sum_{m=0}^{N} b_pH_p - \gamma\sum_{m=0}^{N} c_m\,H_m(t)$$
$$\textstyle\sum_{m=1}^{N} 2mc_mH_{m-1}(t) = \sum_{m=0}^{N} b_pH_p - \gamma\sum_{m=0}^{N} c_m\,H_m(t) \qquad (6)$$
$$\frac{dR}{dt} = \gamma I(t) \Rightarrow \sum_{m=0}^{N} c_mH_m(t)\sum_{p=1}^{N} 2_pd_pH_{p-1}(t) =$$
$$R(t) = \sum_{p=0}^{N} d_pH_p(t)$$
$$\frac{dR}{dt} = \sum_{p=0}^{N} d_p \times 2_pH_{p-1}(t)$$
$$\gamma\textstyle\sum_{m=0}^{N} c_mH_m(t)$$

Integrating (6) by using orthogonally property which state that;

$\int_{-\infty}^{\infty} H_k(t)H(t)e^{-t^2}dt = \sqrt{\pi 2^k k!}\,\delta k_1$ We now multiply LHS and RHS by $H_k(t)e^{-t^2}$ and integrate. $\int_{-\infty}^{\infty}\sum_{n=1}^{N} 2na_nH_{n-1}(t)H_k(t)e^{-t^2}dt = -\beta\int_{-\infty}^{\infty}\sum_{k=0}^{2N} akm_kH_k(t)$

For LHS $=\sqrt{\pi 2^{n-1}}(n-1)!\,\delta_{k,n-1}$

Where; $H_k(t)$ is Hermite polynomial, e^{-t^2} the Gaussian weight function, $H_n(t)$ is the nth Hermite polynomial and δ_{nm} is the kronecker delta function where if n=m &0, if n≠m.

for LHS $\int_{-\infty}^{\infty}\sum_{n=1}^{2N} 2na_nH_{n-1}(t)H_k(t)e^{t^2}dt - \beta\sum_{k=0}^{2N} a_km_k\sqrt{\pi 2^k k!}$

$$\sqrt{\pi 2^k k!}\,a_{k+1} = -\beta\sqrt{\pi 2^k k!}\,a_km_k$$

Integrating $\sum_{p=1}^{N} 2_p b_p H_{p-1}(t) = p\sum_{n=0}^{N}\sum_{m=0}^{N} a_n c_m H_{n+m}(t) - \alpha\sum_{p=0}^{N} b_p H_p(t)$
We now multiply the LHS and RHS by$H_k(t)e^{-t^2}$

$$\int_{-\infty}^{\infty}\sum_{p=1}^{N} 2_p b_p H_{p-1}(t)K_k(t)e^{-t^2} = \int_{-\infty}^{\infty}\left(p\sum_{n=0}^{N}\sum_{n=0}^{N} a_n c_m H_{n+m}(t) - \alpha\sum_{p=0}^{N} b_p H_p(t)\right)H_k(t)e^{-t^2}$$

$$\sqrt{\pi 2^k k!}\,\delta_k! = \frac{1}{2p}a_m c_m \tag{7}$$

$$\int_{-\infty}^{\infty}\sum_{m=1}^{N} 2_m c_m H_{m-1}(t) = \alpha\sum_{p=0}^{N} b_p H_p(t) - \alpha\sum_{m=0}^{N} c_m H_m(t)$$

$$\int_{-\infty}^{\infty}\sum_{m=1}^{N} 2_m c_m H_{m-1}(t)H_k(t)e^{-t^2} = \int_{-\infty}^{\infty}\alpha\left(\sum_{p=0}^{N} b_p H_p(t)H_k(t)e^{-t^2}\right) - \int_{-\infty}^{\infty}\gamma\sum_{m=0}^{N} c_m H_m(t)H_k(t)e^{-t^2}$$

$$\sqrt{\pi 2^{m-1}(m-1)!\,c_m = \sqrt{\pi}\left(\alpha\sum_{p=0}^{N} b_p 2^p p! - \gamma\sum_{m=0}^{N} c_m 2^m m!\right)}$$

$$\sum_{m=1}^{N} 2^m m!\,c_m = \alpha\sum_{m=1}^{N} b_p 2^p p! - \gamma\sum_{m=0}^{N} c_m 2^m m!$$

Integrating $\sum^{N} 2_{pd_pH_{p-1}(t)} \equiv \gamma\sum c_m H_m(t)$

$$\int_{-\infty}^{\infty}\sum_{p=1}^{N} 2_p d_p H_{p-1}\left(te^{-t^2}\right) = \int_{-\infty}^{\infty}\gamma\sum_{m=0}^{N} c_m H_m(t)H_k(t)e^{-t^2}\ \sqrt{\pi}\sum_{p=1}^{N} 2^p\,p!d_p = \gamma\sqrt{\pi}\sum_{m=0}^{N} c_m 2^m m!$$

$\sum^{N} 2^p p!\,d_p = \gamma\sum^{N} c_m 2^m m!$
To apply collocation points andenforce the SEIR model equations at specific points, we use Hermitecollocation pointst_j, where $j = 0,1,2,\ldots\ldots, N$.These are the roots of the Hermitepolynomial$H_{N+1}(t)$.

$$\left.\begin{aligned}
&\sum_{k=0}^{N} c_k^S \frac{dH_k}{dt}|t = t_j = -\beta SI(t_j)\\
&\sum_{k=0}^{N} c_k^E \frac{dH_k}{dt}|t = t_j = \beta SI(t_j) - \alpha E(t)\\
&\sum_{k=0}^{N} c_k^I \frac{dH_k}{dt}|t = t_j = \alpha E(t_j) - \gamma I(t)\\
&\sum_{k=0}^{N} c_k^R \frac{dH_k}{dt}|t = t_j = \gamma I(t_j)
\end{aligned}\right\} \tag{8}$$

Select collocation point's t, where the differential equation will be enforced. These points are typically chosen as the roots of the Hermitepolynomial$H_{N+1}(t)$. Ensuring numerical stability and optimal accuracy.

Formulation the System of Algebraic Equations
At each collocation point t, enforce the SEIR equations;
The system is nonlinear due to terms like$S_N(t)I_N(t)$. To solve it:
Convert to Matrix Form: Express the system as a nonlinear matrix equation:
$A.B = B(C)$
Where:A is a coefficient matrix formed from Hermite polynomials.$C$is the vector of unknown coefficients $C_K^S, C_K^E, C_K^I, C_K^R$.$B(C)$is a vector of nonlinear terms.We use numerical methods Maple 18 for iterative solving reconstructing the Approximate Solutions from Hermite Coefficients in SEIR Model

$$\left.\begin{aligned}
&S_N = C_0^S H_0(t) + c_1^S H_1(t) + \ldots\ldots\ldots\ldots\ldots + c_N^S H_0(t)\\
&E_N = C_0^E H_0(t) + c_1^E H_1(t) + \ldots\ldots\ldots\ldots\ldots + c_N^E H_0(t)\\
&I_N = C_0^I H_0(t) + c_1^I H_1(t) + \ldots\ldots\ldots\ldots\ldots + c_N^I H_0(t)\\
&R_N = C_0^R H_0(t) + c_1^R H_1(t) + \ldots\ldots\ldots\ldots\ldots + c_N^R H_0(t)
\end{aligned}\right\} \tag{9}$$

In this section, to show the accuracy and efficiency of the presented method, the SEIR model of Epidermis model with a potential Application to COVID-19, given in equation(9),is solved .
Solution: The sum of Hermite polynomial for n=3;$a := 0.00003 : b := 0.02 : y := 0.03 : r := 0.01$
General solution of Hermite polynomial defined in equation (9) and Hermite expansion of SEIR
The polynomial series gives;

$$\left.\begin{aligned}
&H_0 = 1\\
&H_1 = 2t\\
&H_2 = 4t^2 - 2\\
&H_3 = 8t^3 - 12t\\
&H_4 = 16t^4 - 48t^2 + 12
\end{aligned}\right\} \tag{10}$$

The general formula gives;$H_n(x) = \frac{(-1)^n d^n}{w(x)dx^n}\{w(x) * g(x)\}S(t) = c_{0,1} + 2c_{1.1}t + c_{2,1}(4t^2 - 2) + c_{3,1}(8t^3 - 12t) + c_{4,1}(16t^4 - 48t^2 + 12)$ (11)
Integrating and Differentiating (11) with initial of S and we obtained;

$S(t) = \frac{16}{5}t^5c_{4,1} + 2t^4c_{3,1} + \left(\frac{4}{3}c_{2,1} - 16c_{4,1}\right)t^3 + (c_{1,1} - 6c_{3,1})t^2 + (c_{0,1} - 2c_{2,1} + 12c_{4,1})t + 40 - S(t) = 16t^4c_{4,1} + 8t^3c_{3,1} + 3\left(\frac{4}{3}c_{2,1} - 16c_{4,1}\right)t^2 + 2(c_{1,1} - 6c_{3,1})t + c_{0,1} - 2c_{2,1} + 12c_{4,1}$ (12)

$E(t) = c_{0,2} + 2c_{1,2}t + c_{2,2}(4t^2 - 2) + c_{3,2}(8t^3 - 12t) + c_{4,2}(16t^4 - 48t^2 + 12)$ (13)

Integrating and Differentiating (13) with initial conditions and we obtain;

$E(t) = \frac{16}{5}t^5c_{4,2} + 2t^4c_{3,2} + \left(\frac{4}{3}c_{2,2} - 16c_{4,2}\right)t^3 + (c_{1,2} - 6c_{3,2})t^2 + (c_{0,2} - 2c_{2,2} + 12c_{4,2})t + 15$

$E(t) = 16t^4c_{4,2} + 8t^3c_{3,2} + 3\left(\frac{4}{3}c_{2,2} - 16c_{4,2}\right)t^2 + 2(c_{1,2} - 6c_{3,2})t + c_{0,2} - 2c_{2,2} + 12c_{4,2}$ (14)

$I(t) = c_{0,3} + 2c_{1,3}t + c_{2,3}(4t^2 - 2) + c_{3,3}(8t^3 - 12t) + c_{4,3}(16t^4 - 48t^2 + 12)$ (15)

Integrating and Differentiating (15) with initial conditions and we obtain

$I(t) = \frac{16}{5} + t^3c_{4,3} + 2t^4c_{3,3} + \left(\frac{4}{3}c_{2,3} - 16c_{4,3}\right)t^3 + (c_{1,3} - 6c_{3,3})t^2 + (c_{0,3} - 2c_{2,3} + 12c_{4,3})t + 10$

$I(t) = 16t^4c_{4,3} + 8t^3c_{3,3} + 3\left(\frac{4}{3}c_{2,3} - 16c_{4,3}\right)t^2 + 2(c_{1,3} - 6c_{3,3})t + c_{0,3} - 2c_{2,3} + 12c_{4,3}$ (16)

$R(t) = c_{0,4} + 2c_{1,4}t + c_{2,4}(4t^2 - 2) + c_{3,4}(8t^3 - 12t) + c_{4,4}(16t^4 - 48t^2 + 12)$ (17)

Integrating and Differentiating (17) with initial conditions and we obtain

$R(t) = \frac{16}{5}t^5c_{4,4} + 2t^4c_{3,4} + \left(\frac{4}{3}c_{2,4} - 16c_{4,4}\right)t^3 + (c_{1,4} - 6c_{3,4})t^2 + (c_{0,4} - 2c_{2,4} + 12c_{4,4})t + 5$

$R(t) = 16t^4c_{4,4} + 8t^3c_{3,4} + 3\left(\frac{4}{3}c_{2,4} - 16c_{4,4}\right)t^2 + 2(c_{1,4} - 6c_{3,4})t + c_{0,4} - 2c_{2,4} + 12c_{4,4}$ (18)

Substituting (12) into (9) and multiplying with the value of parameter $\beta$and we obtain

$$16t^4c_{4,1} + 8t^3c_{3,1} + 3\left(\frac{4}{3}c_{2,1} - 16c_{4,1}\right)t^2 + 2(c_{1,1} - 6c_{3,1})t + c_{0,1} - 2c_{2,1} + 12c_{4,1} =$$
$$-0.01\begin{pmatrix}\frac{16}{5}t^5c_{4,1} + 2t^4c_{3,1} + \left(\frac{4}{3}c_{2,1} - 16c_{4,1}\right)t^3 + (c_{1,1} - 6c_{3,1})t^2 + (c_{0,1} - 2c_{2,1} + 12c_{4,1})t \\ +40\end{pmatrix}$$
$$\begin{pmatrix}\frac{16}{5}t^5c_{4,3} + 2t^4c_{3,3} + \left(\frac{4}{3}c_{2,3} - 2c_{4,3}\right)t^3 + \left(\frac{4}{3}c_{2,3} - 16c_{4,3}\right)t^3 + (c_{1,3} - 6c_{3,3})t^2 \\ +(c_{0,3} - 2c_{2,3} + 12c_{4,3})t + 10\end{pmatrix} \quad (19)$$

Substituting (13) and (9) and multiplying with the parameterα, we have

$$6t^4c_{4,2} + 8t^3c_{3,2} + 3\left(\frac{4}{3}c_{2,2} - 16c_{4,2}\right)t^2 + 2(c_{1,2} - 6c_{3,2})t + 12c_{4,2}$$
$$-0.01\begin{pmatrix}\frac{16}{5}t^5c_{4,1} + 2t^4c_{3,1} + \left(\frac{4}{3}c_{2,1} - 16c_{4,1}\right)t^3 + (c_{1,1} - 6c_{3,1})t^2 + \\ (c_{0,1} - 2c_{2,1} + 12c_{4,1})t + 100\end{pmatrix} \quad (20)$$
$$= \left(\begin{pmatrix}\frac{16}{5}t^5c_{4,3} + 2t^4c_{3,3} + \left(\frac{4}{3}c_{2,3} - 2c_{4,3}\right)t^3 + \left(\frac{4}{3}c_{2,3} - 16c_{4,3}\right)t^3 + (c_{1,3} - 6c_{3,3})t^2 + \\ (c_{0,3} - 2c_{2,3} + 12c_{4,3})t + 10\end{pmatrix}\right)$$
$$-0.06400000000t^5c_{4,2} - 0.04t^4c_{3,2} - 0.03\left(\frac{4}{3}c_{2,2} - 6c_{3,2}\right)t^2 -$$
$$0.02(c_{0,2} - 2c_{2,2} + 12c_{4,2})t - 0.30$$

Substituting (14) and (9) and multiplying with the parameterα, we have

$$\left.\begin{aligned}&16t^4c_{4,3} + 8t^3c_{3,3} + 3\left(\frac{4}{3}c_{2,3} - 16c_{4,3}\right)t^2 + (c_{1,3} - 6c_{3,3})t + c_{0,3} - 2c_{2,3} + 12c_{4,3} \\ &= 0.06400000000t^5c_{4,2} + 0.04t^4c_{3,2} + 0.02\left(\frac{4}{3}c_{2,2} - 16c_{4,2}\right)t^3 + 0.02(c_{1,2} - 6c_{3,2})t^2 \\ &+0.02(c_{0,2} - c_{2,2} + 12c_{4,2})t + 0.150 - 0.04800000000t^5c_{4,3} - 0.030t^4c_{3,3} - \\ &0.015\left(\frac{4}{3}c_{2,3} - 16c_{4,3}\right)t^3 - 0.015(c_{1,3} - 6c_{3,3})t^2 - 0.015(c_{0,3} - 2c_{2,3} + 12c_{4,3})t\end{aligned}\right\} \quad (21)$$

Substituting (15) and (9) and multiplying with the parameter$\alpha$and we obtains;

$$\left.\begin{aligned}&16t^4c_{4,4} + 8t^3c_{3,4} + 3\left(\frac{4}{3}c_{2,4} - 16c_{4,4}\right)t^2 + 2(c_{1,4} - 6c_{3,4})t + c_{0,4} - 2c_{2,4} + 12c_{44} = \\ &0.04800000000t^5c_{4,3} + 0.030t^4c_{3,3} + 0.015\left(\frac{4}{3}c_{2,3} - 16c_{4,3}\right)t^3 + 0.015(c_{1,3} - 6c_{3,3})t^2 \\ &+0.015(c_{0,3} - 2c_{2,3} + 12c_{4,3})t + 0.150\end{aligned}\right\} \quad (22)$$

Collocate of$S(t)$, at t from 0 to 1 and we get;

$c_{0,1} - 2c_{2,1} + 12c_{4,1} = -10.00$ (23)

$$\left.\begin{aligned}&\frac{145}{16}c_{4,1} - \frac{23}{8}c_{3,1} - \frac{7}{4}c_{2,1} + \frac{1}{2}c1,1 + c_{0,1} = \\ &-0.01\left(\frac{881}{320}c_{4,1} - \frac{47}{128}c_{3,1} - \frac{23}{48}c_{2,1} + \frac{1}{16}c_{1,1} + \frac{1}{4}c_{0,1} + 40\right) \\ &\left(\frac{881}{320}c_{4,3} - \frac{47}{128}c_{3,3} - \frac{23}{48}c_{2,3} + \frac{1}{16}c_{1,3} + \frac{1}{4}c_{0,3} + 10\right)\end{aligned}\right\} \quad (24)$$

$$\left.\begin{aligned}&c_{4,1}-5c_{3,1}-c_{2,1}+c_{1,1}+c_{0,1}=\\&-0.01\left(\frac{41}{10}c_{4,1}-\frac{11}{8}c_{3,1}-\frac{5}{6}c_{2,1}+\frac{1}{4}c_{1,1}+\frac{1}{2}c_{0,1}+40\right)\\&\left(\frac{41}{10}c_{4,3}-\frac{11}{8}c_{3,3}-\frac{5}{6}c_{2,3}+\frac{1}{4}c_{1,3}+\frac{1}{2}c_{0,3}+10\right)\end{aligned}\right\} \quad (25)$$

$$\left.\begin{aligned}&-\tfrac{159}{16}c_{4,1}-\tfrac{45}{8}c_{3,1}+\tfrac{1}{4}c_{2,1}+\tfrac{3}{2}c_{1,1}+c_{0,1}=\\&-0.01\left(\tfrac{963}{320}c_{4,1}-\tfrac{351}{128}c_{3,1}-\tfrac{15}{16}c_{2,1}+\tfrac{9}{16}c_{2,1}+\tfrac{3}{4}c_{0,1}+40\right)\\&\left(\tfrac{963}{320}c_{4,3}-\tfrac{351}{128}c_{3,3}-\tfrac{15}{16}c_{2,3}+\tfrac{9}{16}c_{1,3}+\tfrac{3}{4}c_{0,3}+10\right)\end{aligned}\right\} \quad (26)$$

$$\left.\begin{aligned}&-20c_{4,1}-4c_{3,1}+2c_{2,1}+2c_{1,1}+c_{0,1}=\\&-0.01\left(-\tfrac{4}{5}c_{4,1}-4c_{3,1}-\tfrac{2}{3}c_{2,1}+c_{1,1}+c_{0,1}+40\right)\\&\left(-\tfrac{4}{5}c_{4,3}-4c_{3,3}-\tfrac{2}{3}c_{2,3}+c_{1,3}+c_{0,3}+10\right)\end{aligned}\right\} \quad (27)$$

Collocate of $E(t)$, at t from 0 to 1 and we get;

$$c_{0,2}-2c_{2,2}+12c_{4,2}=9.70 \quad (28)$$

$$\left.\begin{aligned}&\tfrac{145}{16}c_{4,2}-\tfrac{23}{8}c_{3,2}-\tfrac{7}{4}c_{2,2}+\tfrac{1}{2}c_{1,2}+c_{0,2}=0.01\begin{pmatrix}\tfrac{881}{320}c_{4,1}-\tfrac{47}{128}c_{3,1}-\tfrac{23}{48}c_{2,1}\\+\tfrac{1}{16}c_{1,1}+\tfrac{1}{4}c_{0,1}+100\end{pmatrix}\\&\left(\tfrac{881}{320}c_{4,3}-\tfrac{47}{128}c_{3,3}-\tfrac{23}{48}c_{2,3}+\tfrac{1}{16}c_{1,3}+\tfrac{1}{4}c_{0,3}+10\right)-0.05506250000c_{4,2}\\&+0.007343750000c_{3,2}+0.009583333333c_{2,2}-0.001250000000c_{1,2}\\&-0.005000000000c_{0,2}-0.30\end{aligned}\right\} \quad (29)$$

$$\left.\begin{aligned}&c_{4,2}-5c_{3,2}-c_{2,2}+c_{1,2}+c_{0,2}=\\&001\left(\tfrac{41}{10}c_{4,1}-\tfrac{11}{8}c_{3,1}-\tfrac{5}{6}c_{2,1}+\tfrac{1}{4}c_{1,1}+\tfrac{1}{2}c_{0,1}+40\right)\\&\left(\tfrac{41}{10}c_{4,4}-\tfrac{11}{8}c_{3,3}-\tfrac{5}{6}c_{2_3}+\tfrac{1}{4}c_{1,3}+\tfrac{1}{2}c_{0,3}+10\right)-0.0820000000c_{4,2}\\&+0.027500000000c_{3,2}+0.01666666667c_{2,2}-0.005000000000c_{1,2}\\&-0.01000000000000c_{0,2}-0.30\end{aligned}\right\} \quad (30)$$

$$\left.\begin{aligned}&-\tfrac{159}{16}c_{4,2}-\tfrac{45}{8}c_{3,2}+\tfrac{1}{4}c_{2,2}+\tfrac{3}{2}c_{1,2}+c_{0,2}=\\&0.01\left(\tfrac{963}{320}c_{4,1}-\tfrac{351}{128}c_{3,1}-\tfrac{15}{16}c_{2,1}+\tfrac{9}{16}c_{1,1}+\tfrac{3}{4}c_{0,1}+40\right)\\&\left(\tfrac{963}{320}c_{4,3}-\tfrac{351}{128}c_{3,3}-\tfrac{15}{16}c_{2,3}+\tfrac{9}{16}c_{1,3}+\tfrac{3}{4}c_{0,3}+10\right)-0.0601875000c_{4,2}\\&+0.05484375000c_{3,2}+0.01875000000c_{2,2}-0.01125000000c_{1,2}\\&-0.015000000000c_{0,2}-0.30\end{aligned}\right\} \quad (31)$$

$$\left.\begin{aligned}&-20c_{4,2}-4c_{3,2}+2c_{2,2}+2c_{1,2}+c_{0,2}=\left(-\tfrac{4}{5}c_{4,1}-4c_{3,1}-\tfrac{2}{3}c_{2,1}+c_{1,1}+40\right)\\&\left(-\tfrac{4}{5}c_{4,3}-4c_{3,3}-\tfrac{2}{3}c_{3,2}+c_{1_{3,1}}+10\right)+0.0160000000c_{4,2}+0.08c_{3,2}+\\&0.01333333333c_{2,2}-0.02c_{1,2}-0.02c_{0,2}-0.30\end{aligned}\right\} \quad (32)$$

Collocate of $I(t)$, at t from 0 to 1 and we get;

$$c_{0,3}-2c_{2,3}+12c_{4,3}=0.150$$

$$\frac{145}{16}{}_{3,3}-\frac{23}{8}c_{2,3}-\frac{7}{4}c_{2,3}+\frac{1}{2}c_{1,3}+c_{0,3}=0.05506250000c_{4,2}-$$

$$0.007343750000c_{3,2}-0.009583333333c_{2,2}+0.001250000000c_{1,2} \quad (33)$$

$$\left.\begin{aligned}&+0.005000000000c_{0,2}+0.150-0.04129687500c_{4,3}+0.05507812500c_{3,3}\\&+0.0071875000000c_{2,3}-0.0009375000000c_{1,3}-0.003750000000c_{0,3}\end{aligned}\right\} \quad (34)$$

$$\left.\begin{aligned}&-\tfrac{159}{16}c_{4,3}-\tfrac{45}{8}c_{3,3}+\tfrac{1}{4}c_{2,3}+\tfrac{3}{2}c_{1,3}+c_{0,3}=0.0601875000c_{4,2}-\\&0.05484375000c_{3,2}-0.01875000000c_{2,2}+0.01125000000c_{1,2}\\&+0.01500000000c_{0,2}+0.150-0.0451406250c_{4,3}+0.04113281250c_{3,3}\\&+0.01406250000c_{2,3}-0.008437500000c_{1,3}-0.01125000000c_{0,3}\end{aligned}\right\} \quad (35)$$

$$\left.\begin{aligned}&-20c_{4,3}-4c_{3,3}+2c_{2,3}+2c_{1,3}+c_{0,3}=-0.0160000000c_{4,2}-0.08c_{3,2}-\\&0.01333333333c_{2,2}+0.02c_{1,2}+0.02c_{0,2}+0.150+0.0120000000c_{2,3}\\&-0.015c_{1,3}-0.015c_{0,3}\end{aligned}\right\} \quad (36)$$

Collocate of $R(t)$, at t from 0 to 1 and we get;

$$c_{0,4}-2c_{2,4}+12c_{4,4}=0.150 \quad (37)$$

$$\left.\begin{array}{l}\frac{145}{16}c_{4,4}-\frac{23}{8}c_{3,4}-\frac{7}{4}c_{2,4}+\frac{1}{2}c_{1,4}+c_{0,4}=0.04129687500c_{4,3}\\-0.005507812500c_{3,3}-0.007187500000c_{2,3}+0.00093750000000c_{1,3}\\+0.0037500000000c_{0,3}+0.150\end{array}\right\} \quad (38)$$

$$\left.\begin{array}{l}c_{4,4}-5c_{3,4}-c_{2,4}+c_{1,4}+c_{0,4}=0.06150000000c_{4,3}-\\0.02062500000c_{3,3}-0.0125000000000c_{2,3}+0.003750000000c_{1,3}\\+0.007500000000c_{0,3}+0.0150\end{array}\right\} \quad (39)$$

$$\left.\begin{array}{l}-\frac{159}{16}c_{4,4}-\frac{45}{8}c_{3,4}+\frac{1}{4}c_{2,4}+\frac{3}{2}c_{1,4}+c_{0,4}=0.0451406250c_{4,3}-\\0.04113281250c_{3,3}-0.01406250000c_{2,3}+0.008437500000c_{1,3}\\+0.01125000000c_{0,3}+0.150\end{array}\right\} \quad (40)$$

$$\left.\begin{array}{l}-20c_{4,4}-4c_{3,4}+2c_{2,4}+2c_{1,4}+c_{0,4}=-0.0120000000c_{4,3}-0.060c_{3,3}\\-0.01000000000c_{2,3}+0.015c_{1,3}+0.015c_{0,3}\end{array}\right\} \quad (41)$$

Simplifying we have;

$$\left.\begin{array}{l}c_{0,1}=-0.3360538699, c_{0,2}=-0.8641713587, c_{0,3}=0.1000855608, c_{0,4}=0.1001146675\\c_{1,1}=-5.840470700\times10^{7}, c_{1,2}=5.823195871\times10^{7}, c_{1,3}=86414.11133, c_{1,4}=86334.17912\\c_{2,1}=4.639825355\times10^{7}, c_{2,2}=-4.627136304\times10^{7}, c_{2,3}=-63473.27731, c_{2,4}=-63417.23325\\c_{3,1}=-9.363577801\times10^{6}, c_{3,2}=9.336361522\times10^{6}, c_{3,3}=13614.28799, c_{3,4}=13601.99125\\c_{4,1}=3.164578756\times10^{6}, c_{4,2}=-3.156366554\times10^{6}, c_{4,3}=-4107.859432, c_{4,4}=-4104.342424\end{array}\right\} \quad (42)$$

We obtain approximate solution:

$$\left.\begin{array}{l}Sr=40-0.3360000000t+0.002849599994t^{2}-0.00003590604954t^{3}+\\3.6532651227\times10^{-7}t^{4}-2.899165674\times10^{-9}t^{5}\end{array}\right\} \quad (43)$$

$$\left.\begin{array}{l}Er=30-0.8640000000+0.01229040000t^{2}-0.0001142299033t^{3}+\\7.649042588\times10^{-7}t^{4}-3.680365651\times10^{-9}t^{5}\end{array}\right\} \quad (44)$$

$$\begin{array}{l}20.0000570+0.09999999998t-0.004819999997t^{2}-4.281283742\times10^{-7}\\+2.33388417\times10^{-7}\end{array} \quad (45)$$

$$\left.\begin{array}{l}10+0.100000000t-0.005319999994t^{2}+0.00007643463547t^{3}-\\6.676825248\times10^{-7}t^{4}+4.140731674\times10^{-9}t^{5}\end{array}\right\} \quad (46)$$

Application of Laplace Adomian Decomposition Method (LADM)

By applying Laplace Adomian Decomposition method on model (3)

Where$\chi_t{}^{\eta} 0 \le \eta \le 1$ is the Non-integer fractional order,ηdemonstrate the fractional time order, we perform a Laplace transform in equation (3), resulting in the following:

$$\begin{array}{l}L\{{}^{c}\chi^{\eta}S(t)\}=L\{-\beta S(t)I(t)\},\\L\{{}^{c}\chi^{\eta}E(t)\}=L\{\beta S(t)I(t)-\alpha E(t)\},\\L\{{}^{c}\chi^{\eta}I(t)\}=L\{\alpha E(t)-\gamma I(t)\},\\L\{{}^{c}\chi^{\eta}R(t)\}=L\{\gamma I(t)\},\end{array} \quad (47)$$

Initial condition$S_0=x_1, E_0=x_2, I_0=x_3, R_0=x_4$.

Laplace's transform definition gives us

$$\begin{array}{l}v^{\eta}L\{S(t)\}-v^{\eta-1}S(0)=L\{-\beta S(t)I(t)\}\\v^{\eta}L\{E(t)\}-v^{\eta-1}E(0)=L\{\beta S(t)I(t)-\alpha E(t)\}\\v^{\eta}L\{I(t)\}-v^{\eta-1}I(0)=L\{\alpha E(t)-\gamma I(t)\}\\v^{\eta}L\{R(t)\}-v^{\eta-1}R(0)=L\{\gamma I(t)\}\end{array} \quad (48)$$

Simplify (48)

$$\begin{array}{l}v^{\eta}L\{S(t)\}=v^{\eta-1}S(0)+L\{-\beta S(t)I(t)\}\\v^{\eta}L\{E(t)\}=v^{\eta-1}E(0)+L\{\beta S(t)I(t)-\alpha E(t)\}\\v^{\eta}L\{I(t)\}=v^{\eta-1}I(0)+L\{\alpha E(t)-\gamma I(t)\}\end{array} \quad (49)$$

We derive the equation from the initial condition. (49)

$$\begin{array}{l}S(t)=\frac{x_1}{v}+\frac{1}{v^{\eta}}L\{-\beta S(t)I(t)\}\\E(t)=\frac{x_1}{v}+\frac{1}{v^{\eta}}L\{\beta S(t)I(t)-\alpha E(t)\}\\I(t)=\frac{x_1}{v}+\frac{1}{v^{\eta}}L\{\alpha E(t)-\gamma I(t)\}\end{array} \quad (50)$$

Considering that the technique provides an infinite series solution,

$$S(t)=\sum_{n=0}^{\propto}S_n, E(t)=\sum_{n=0}^{\propto}E_n, . I(t)=\sum_{n=0}^{\propto}I_n, . R(t)=\sum_{n=0}^{\propto}R_n,$$

The nonlinear term involved $I(t)S(t)$ can be expressed as

$$I(t)S(t)=\sum_{n=0}^{\propto}X_n, \quad (51)$$

WhereZ_nAdomain polynomials provided by

$$Z_n=\frac{1}{\Gamma(n+1)}\frac{d^n}{dt}[\sum_{k=o}^{n} \quad \lambda^k I_K \sum_{k=0}^{n}\lambda^n S_k]\lambda \quad (52)$$

Substitute equations (51) and (52) into (50), we get

$$S(t)=\frac{x_1}{v}+\frac{1}{v^{\eta}}L\{-\beta Z_n\}$$

$$E(t)=\frac{x_1}{v}+\frac{1}{v^{\eta}}L\{Z_n-\alpha E_n\}$$

$I(t) = \frac{x_1}{v} + \frac{1}{v^\eta} L\{\alpha E_n - \gamma I_n\}$
$R(t) = \frac{x_1}{v} + \frac{1}{v^\eta} L\{\gamma I_n\}$ (53)

We apply the term in equation (53) repeatedly and then use Laplace inversion to get the solution for every compartment, which gives us the whole model formula.

$\sum_{n=0}^{\infty} S_{n+1}(t) = L^{-1}[\frac{1}{v^\eta} L\{-\beta Z_n\}]$
$\sum_{n=0}^{\infty} E_{n+1}(t) = L^{-1}[\frac{1}{v^\eta} L\{Z_n - \alpha E_n\}]$
$\sum_{n=0}^{\infty} I_{n+1}(t) = L^{-1}[\frac{1}{v^\eta} L\{\alpha E_n - \gamma I_n\}]$
$\sum_{n=0}^{\infty} R_{n+1}(t) = L^{-1}[\frac{1}{v^\eta} L\{\gamma I_n\}]$ (54)

The followings were obtained from (54);
$S_0 = x_1, E_0 = x_2, I_0 = x_3, R_0 = x_4.$ (55)
$S_1 = (-\beta x_1 x_3)\frac{t^{\eta_1}}{\Gamma(\eta_1+1)}.$
$E_1 = (-\beta x_1 x_3 - \alpha x_2)\frac{t^{\eta_1}}{\Gamma(\eta_1+1)}.$
$I_1 = (\alpha x_2 - \alpha x_2)\frac{t^{\eta_1}}{\Gamma(\eta_1+1)}$
$R_1 = (\gamma x_4)\frac{t^{\eta_1}}{\Gamma(\eta_1+1)}.$ (56)
$S_2 = \beta((x_3 - \beta x_1 x_3)\frac{t^{2\eta_1}}{\Gamma(2\eta_1+1)} + x_1(\alpha x_2 - \alpha x_2)\frac{t^{2\eta_1}}{\Gamma(2\eta_1+1)})$
$E_2 = \beta((x_3 - \beta x_1 x_3)\frac{t^{2\eta_1}}{\Gamma(2\eta_1+1)} + x_1(\alpha x_2 - \alpha x_2)\frac{t^{2\eta_1}}{\Gamma(2\eta_1+1)}) - \alpha(-\beta x_1 x_3 - \alpha x_2)\frac{t^{2\eta_1}}{\Gamma(2\eta_1+1)}.$
$I_2 = \alpha(-\beta x_1 x_3 - \alpha x_2)\frac{t^{2\eta_1}}{\Gamma(2\eta_1+1)} - \gamma(\alpha x_2 - \gamma x_3)\frac{t^{2\eta_1}}{\Gamma(2\eta_1+1)}$
$R_2 = \gamma(\gamma x_4)\frac{t^{2\eta_1}}{\Gamma(2\eta_1+1)}$ (57)

RESULTS AND DISCUSSION

Numerical Results

To illustrate the effectiveness of HCM and LADM numerical computations were carried out using Maple software with Variable values:$S(0) = 20, E(0) = 18, I(0) = 15, R(0) = 10$ and parameter values β=0.01,α=0.03, γ=0.02.

The collocation method transforms the SEIR system into nonlinear algebraic equations for the unknown Hermite coefficients, yielding accurate approximate solutions. The Laplace transform converts derivatives into algebraic expressions, while Adomian polynomials handle nonlinear terms. Applying the inverse Laplace transform provides a series solution. LADM efficiently solves differential equations, offering rapid convergence without discretization. Simulations explore the impact of parameters on disease transmission and progression. The tables below give analysis generated from results:The results of absolute error in HCM numerical computations are shown in Table 1. Absolute error computations using HCM are provided in Table 2. Table 3 presents the absolute errors in the numerical computation of the susceptible population $S(t)$ using HCM and LADM methods. The absolute errors in the exposed population $E(t)$ using HCM and LADM are summarized in Table 4. Table 5 displays the absolute errors in the infected population $I(t)$ using HCM and LADM computations. The absolute errors in the recovered population $R(t)$ using HCM and LADM are given in Table 6. Figure 1 illustrates the changes in the susceptible population over time. Figure 2 illustrates the progression of the exposed population over time. The changes in the infected population as the epidemic progresses are shown in Figure 3. Figure 4 demonstrates the increase in the recovered population throughout the epidemic. Figure 5 provides a consolidated view of how all SEIR model variables interact over time .The impact of parameter variations on disease transmission is analyzed in Figure 6.The comparison of numerical simulations is depicted in Figure 7. Figure 8 shows the exposed population trends over time. The peak infections and transitions among different compartments are demonstrated in Figure 9. Figure 10 provides a combined view of all SEIR model variables, offering a comprehensive perspective on epidemic dynamics. Figure 11 presents the comparative analysis of different numerical solution approaches applied to the SEIR model. Figure 12 evaluates the numerical stability of the model. The recovery trends in the population are analyzed in Figure 14.

Error Estimation

The accuracy of the method is assessed by substituting the approximate solutions into the original SEIR equations and computing the residual error:

Error$=\left|\frac{dS}{dt} + \beta SI(t)\right| + \left|\frac{dE}{dt} - \beta SI(t) + \alpha E(t)\right| + \left|\frac{dI}{dt} - \alpha E(t) + \gamma I(t)\right| + \left|\frac{dR}{dt} - \gamma I(t)\right|$

The truncation limit N is increased until the error satisfies a predefined tolerance.

HCM numerical computations

$S(t) = 20 - 3.000000000t + 0.2004531635t^2 - 0.08804542876t^3$
$E(t) = 18 + 2.460000000t - 2.2372705730t^2 + 0.01101206759t^3$
$I(t) = 15 + 0.2400000000t + 0.03440534566t^2 - 0.002052413108t^3$
$R(t) = 10 + 0.3000000000t + 0.002412063830t^2 + 0.002052413108t^3$

LADM numerical computations

$S(t) = 20 - 3.00t + 0.20100000t^2$
$E(t) = 18 + 2.46t - 0.2379000000t^2$
$I(t) = 25 + 0.24t + 0.03450000t^2$
$R(t) = 10 + 0.30t - 0.00240000t^2$

Table 1: The Values of Absolute Error $S(t), E(t), I(t), R(t)$. in HCM Numerical Computations

t	S(t)	E(t)	I(t)	R(t)
0.1	19.70199573	18.24363831	15.02434164	10.03002433
0.2	19.40794769	18.48259727	15.04935691	10.06009812
0.3	19.11780306	18.71694297	15.07503134	10.09022263
0.4	18.83150902	18.94674148	15.10135044	10.12039907
0.5	18.54901272	19.17205886	15.12829974	10.15062867
0.6	18.27026136	19.39296120	15.15586477	10.18091268
0.7	17.99520209	19.60951456	15.18403104	10.21125231
0.8	17.72378210	19.82178501	15.21278408	10.24164880
0.9	17.45594855	20.02983863	15.24210942	10.27210339
1.0	17.19164862	20.23374150	15.27199258	10.30261731

Table 2: The Values of Absolute Error $S(t), E(t), I(t), R(t)$. in HCM Numerical Computations

t	S(t)	E(t)	I(t)	R(t)
0.1	19.70201000	18.24362100	15.02434500	10.02997600
0.2	19.40804000	18.48248400	15.04938000	10.05990400
0.3	19.11809000	18.48248400	15.07510500	10.08978400
0.4	18.83216000	18.94593600	15.10152000	10.11961600
0.5	18.55025000	19.17052500	15.12862500	10.14940000
0.6	18.27236000	19.39035600	15.15642000	10.17913600
0.7	17.99849000	19.60542900	15.18490500	10.20882400
0.8	17.72864000	19.81574400	15.21408000	10.23846400
0.9	17.46281000	20.02130100	15.24394500	10.26805600
1.0	17.46281000	20.22210000	15.27450000	10.29760000

Table 3: The Values of Absolute Error$S(t)$ in HCM and LADM Numerical Computations

t	SR1	SR2	SR3	SR(LADM)	Abs(sr2-sr1)	Abs(sr3-sr2)
0.1	19.70187648	19.70199573	19.70203444	19.70201000	0.00011925	0.00003871
0.2	19.40750592	19.40794769	19.40809894	19.40804000	0.00044177	0.00015125
0.3	19.11688833	19.11780306	19.40809894	19.11809000	0.00091473	0.00033317
0.4	18.83002369	18.83150902	18.83209033	18.83216000	0.00148533	0.00058131
0.5	18.54691202	18.54901272	18.54990652	18.55025000	0.00210070	0.00089380
0.6	18.26755330	18.27026136	18.27153137	18.27236000	0.00270806	0.00127001
0.7	17.99194755	17.99520209	17.99691273	17.99849000	0.00325454	0.00171064
0.8	17.72009476	17.72378210	17.72599974	17.72864000	0.00368734	0.00221764
0.9	17.45199493	17.45594855	17.45874280	17.46281000	0.00395362	0.00279425
1.0	17.18764806	17.19164862	17.19509361	17.20100000	0.00400056	0.00344499

Table 4: The Values of Absolute Error $E(t)$ in HCM and LADM Numerical Computations

T	Er1	Er2	Er3	Er(LADM)	Abs(Er2-Er1)	Abs(Er3-Er2)
0.1	18.24378770	18.24363831	18.24363342	18.24362100	0.00014939	0.00000489
0.2	18.48315082	18.48259727	18.48258189	18.48248400	0.00055355	0.00001538
0.3	18.71808933	18.71694297	18.71691661	18.71658900	0.00114636	0.00002636
0.4	18.94860326	18.94674148	18.94670730	18.94593600	0.00186178	0.00003418
0.5	19.17469260	19.17205886	19.17202221	19.17052500	0.00263374	0.00003665
0.6	19.39635734	19.39296120	19.39292809	19.39035600	0.00339614	0.00003311
0.7	19.61359749	19.60951456	19.60949025	19.60542900	0.00408293	0.00002431
0.8	19.82641304	19.82178501	19.82177247	19.81574400	0.00462803	0.00001254
0.9	20.03480401	20.02983863	20.02983711	20.02130100	0.00496538	0.00000152
1.0	20.23877038	20.23374150	20.23374500	20.22210000	0.00502888	0.00000350

Table 5: The Values of Absolute Error $I(t)$ in HCM and LADM Numerical Computations

T	Ir1	Ir2	Ir3	Ir(LADM)	Abs(ir2-ir2)	Abs(ir3-ir2)
0.1	15.02430873	15.02434164	15.02434239	15.02434500	0.00003291	$7.5\ 10^{-7}$
0.2	15.04923491	15.04935691	15.04935926	15.04938000	0.00012200	0.00000235
0.3	15.07477855	15.07503134	15.07503535	15.07510500	0.00025279	0.00000401
0.4	15.10093965	15.10135044	15.10135563	15.10152000	0.00041079	0.00000519
0.5	15.12771821	15.12829974	15.12830529	15.12862500	0.00058153	0.00000519
0.6	15.15511422	15.15586477	15.15586975	15.15642000	0.00075055	0.00000498
0.7	15.18312769	15.18403104	15.18403465	15.18490500	0.00090335	0.00000361
.8	15.21175861	15.21278408	15.21278587	15.21408000	0.00102547	0.00000179
0.9	15.24100699	15.24210942	15.24210951	15.24394500	0.00110243	9.10^{-8}
1.0	15.27087283	15.27199258	15.27199189	15.27450000	0.00111975	$6.9\ 10^{-7}$

Table6: The Values of Absolute Error $R(t)$ in HCM and LADM Numerical Computations

T	Rr1	Rr2	Rr3	Rr(LADM)	Abs(Rr2- Rr1)	Abs(Rr3- Rr2)
0.1	10.03622388	10.03624398	10.03624441	10.02997600	0.00002010	$4.3\ 10^{-7}$
0.2	10.07289551	10.07297002	10.07297139	10.05990400	0.00007451	0.00000137
0.3	10.11001489	10.11016931	10.11017164	10.08978400	0.00015442	0.00000233
0.4	10.14758203	10.14783300	10.14783602	10.11961600	0.00025097	0.00000302
0.5	10.18559693	10.18595227	10.18595549	10.14940000	0.00035534	0.00000322
0.6	10.22405957	10.22451829	10.22452118	10.17913600	0.00045872	0.00000289
0.7	10.26296997	10.26352223	10.26352432	10.20882400	0.00055226	0.00000209
0.8	10.30232813	10.30295526	10.30295628	10.23846400	0.00062713	0.00000102
0.9	10.34213404	10.34280854	10.34280858	10.26805600	0.00067450	$4.\ 10^{-8}$
1.0	10.38238770	10.38307326	10.38307284	10.29760000	0.00068556	$4.2\ 10^{-7}$

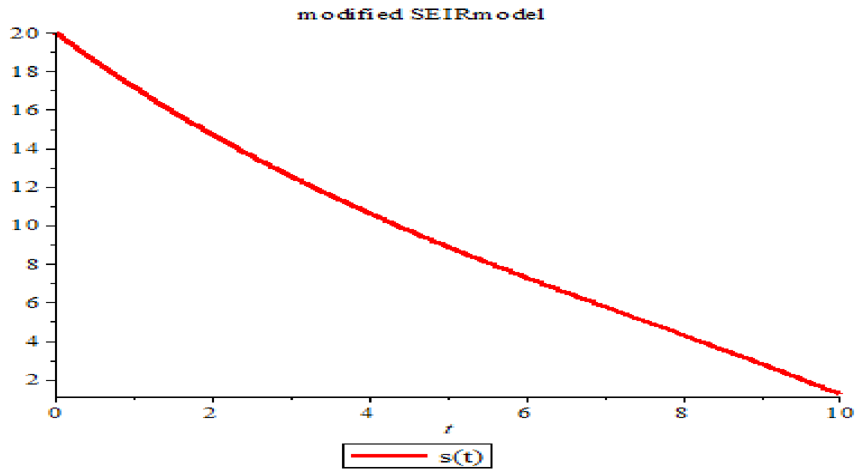

Figure 1: Temporal Changes in the Susceptible Population Under the Fractional-Order SEIR Model

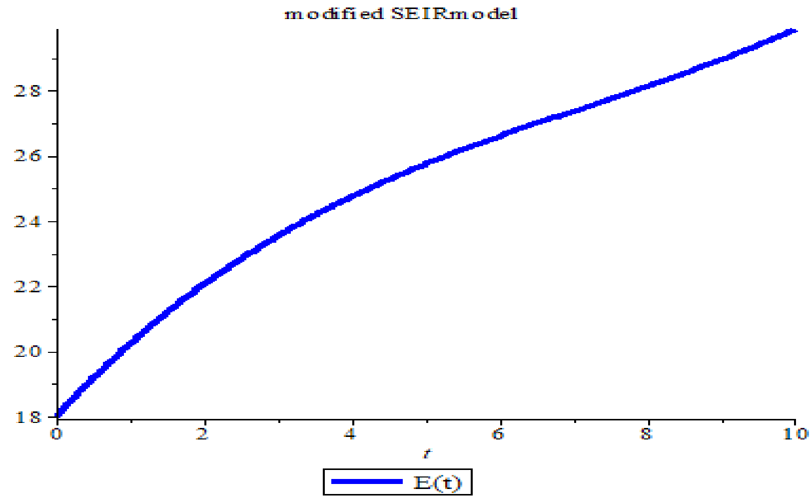

Figure 2: Dynamics of the Exposed Population during Epidemic Progression

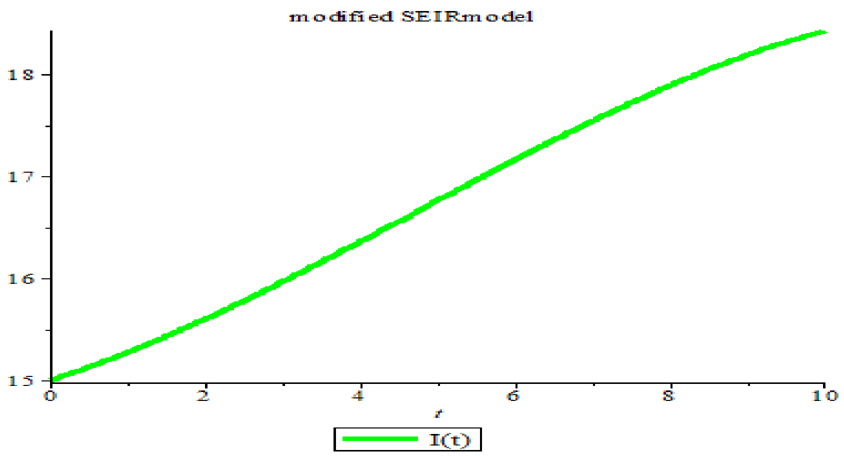

Figure 3: Evolution of the Infected Population over Time using Fractional-Order SEIR Model

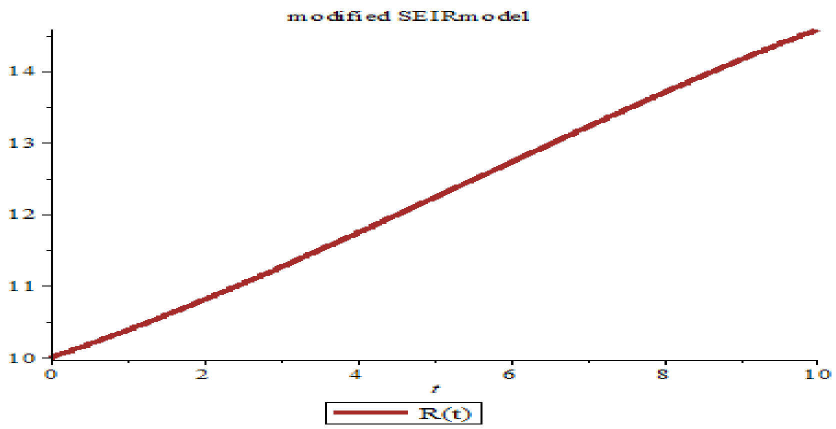

Figure 4: Recovery Trends in the Population Throughout the Epidemic Period

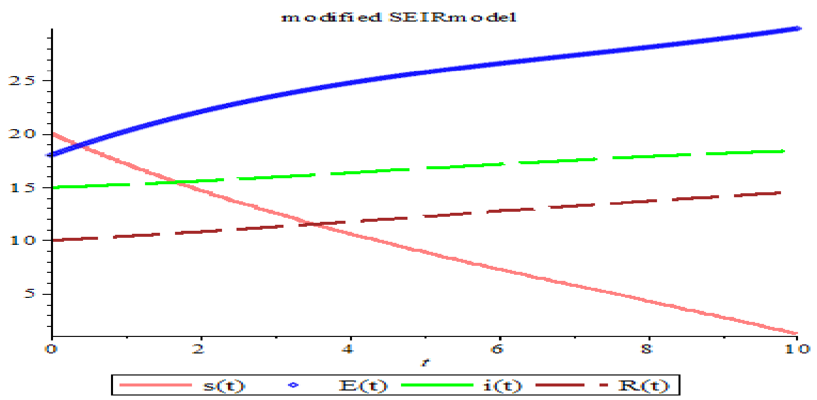

Figure 5: Consolidated Dynamics of Susceptible, Exposed, Infected, and Recovered Populations in the SEIR Model

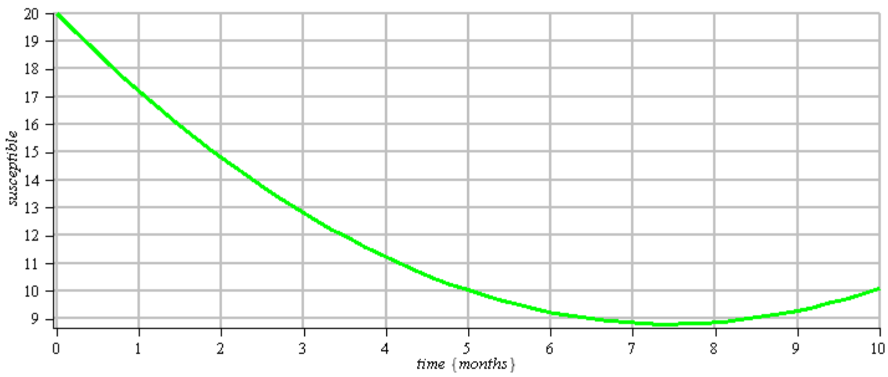

Figure 6: Impact of Parameter Variations on Transmission and Epidemic Dynamics

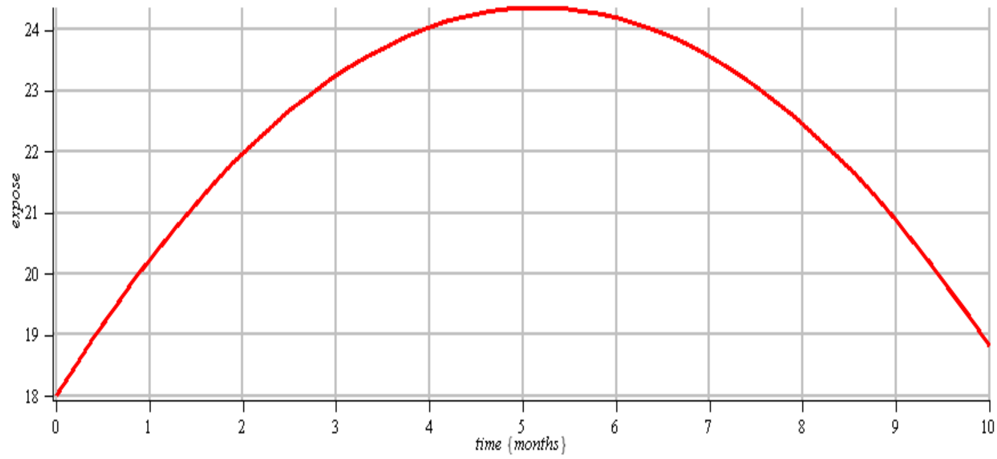

Figure 7: Comparative Numerical Simulations of SEIR Dynamics using HCM and LADM

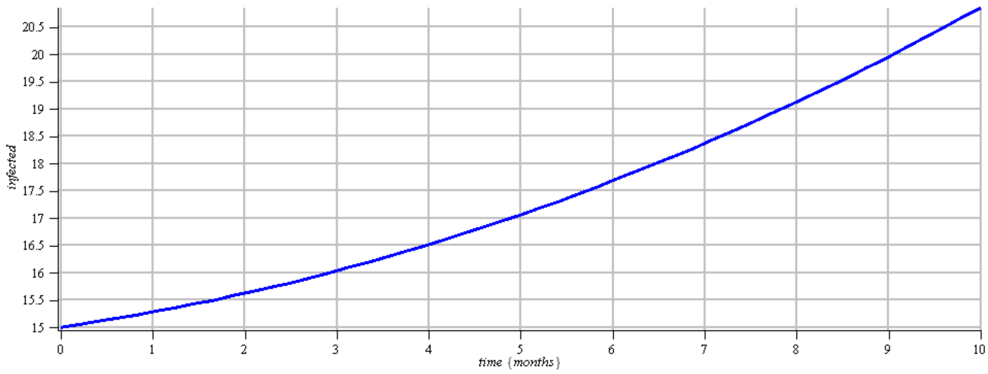

Figure 8: Infected Population Trends over Time across Numerical Simulations

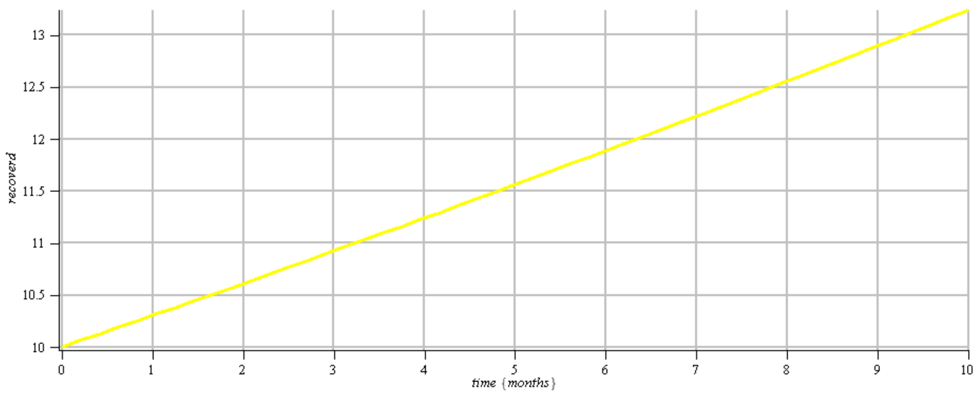

Figure 9: Peak Infection Levels and Transitions among SEIR Compartments

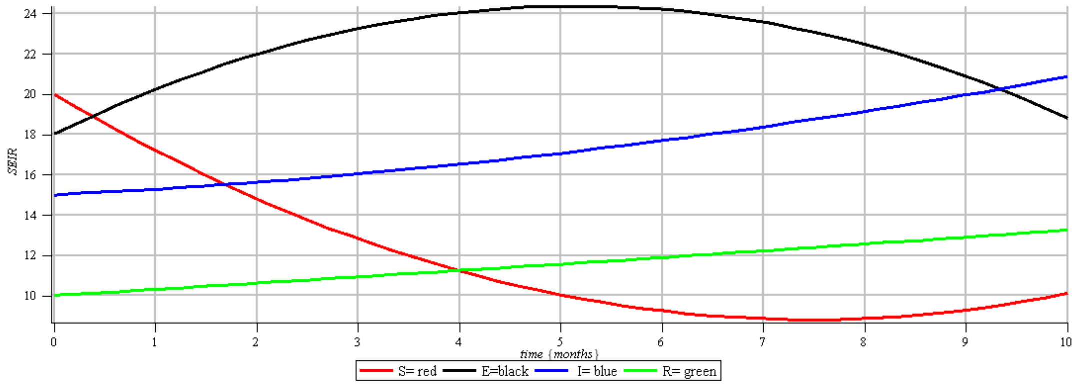

Figure 10: Combined Representation of SEIR Model Variables Illustrating Epidemic Progression

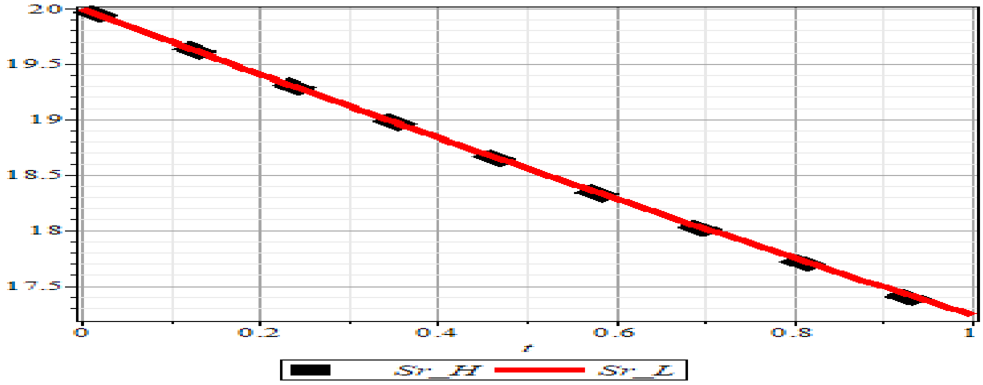

Figure 11: Comparative Performance Analysis of HCM and LADM in Solving the SEIR Model

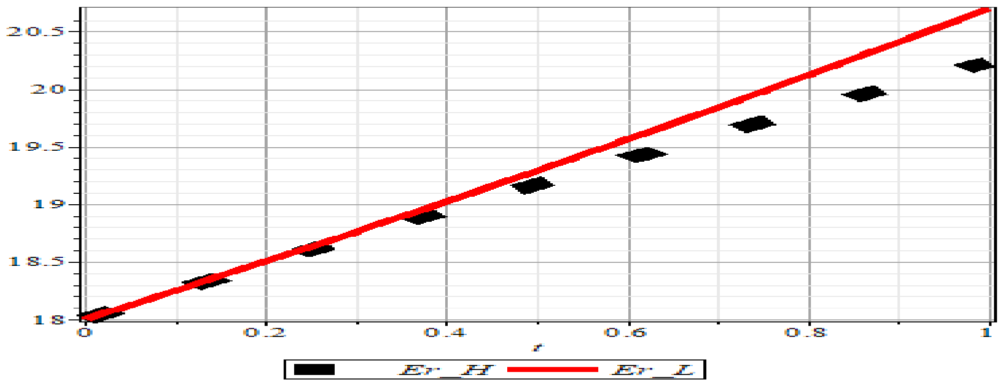

Figure 12: Evaluation of Numerical Stability for Fractional-Order SEIR Model Solutions

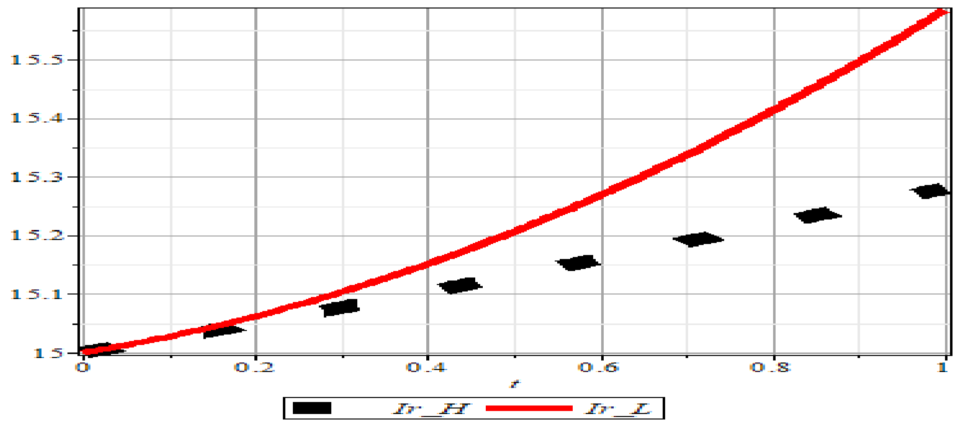

Figure 13: Comparative Temporal Changes of SEIR Compartments using HCM (red line) and LADM (Black dash line)

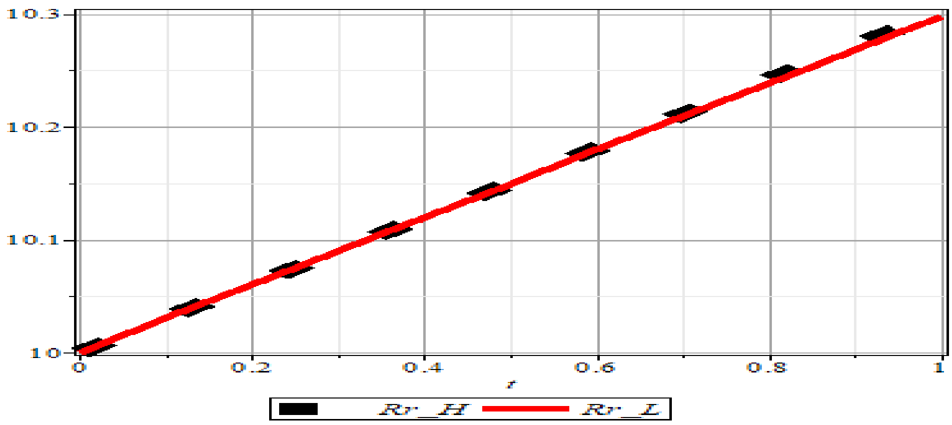

Figure 14: Recovery Dynamics Illustrating Long-Term Epidemic Outcomes under Fractional-Order Modeling

Discussion

The comparison of the dynamics of epidemics based on the fractional-order SEIR model employed with Hermite Collocation Method (HCM) and Laplace-Adomian Decomposition Method (LADM) gives a full picture of the dynamics of epidemics, as they are able to describe the temporal changes of the susceptible population, the exposed population, the infected population, and the recovered population. As shown in Figures 1-4, the anticipated compartmental transitions are a decreasing number of susceptibles as one becomes an exposed individual, an increase and peak in the exposed and infected compartments as an individual becomes a disease host, and a steady increase in the number of recovered individuals as they recover. All these compartments are summarized in Figure 5 due to the interdependence, although Figure 6 illustrates sensitivity of epidemic outcomes to essential parameters like the rate of transmission, incubation period and recovery rate. These findings demonstrate that the effects of parameter changes on the intensity and timing of an epidemic are drastic, which supports the fact that model calibration is essential in correct prediction. Figures 7-14 compare the efficiency in numbers and precision with which HCM and LADM solved the SEIR system. Figures 11-13 indicate that HCM solutions (red line) follow epidemic trends more accurately, and LADM (black markers) generates slight deviations, but still upholds the general forecasts. Figure 14 also indicates long-term recovery results with the use of the fractional-order modeling, with the help of highlighting the effect of memory effects in enhancing predictive realism. Overall, this evidence shows that HCM and LADM are both effective, HCM is more precise and stable, which is why it is a better instrument to evaluate epidemic processes and create the most appropriate solution to such problems as the development of vaccination and control measures over the disease.

CONCLUSION

People face major health dangers from COVID-19 because the virus spreads quickly between people. The research applies a Caputo fractional SEIR model which helps analyze SARS-CoV-2 variant transmission while evaluating control strategies. The Exposed compartment addition in the model improves both disease transmission understanding and predictions regarding variant development patterns.The analysis of the model's nonlinear equations involves testing two advanced approximation solutions namely Hermite Collocation Method (HCM) and Laplace-Adomian Decomposition Method (LADM). The extensive complexity of this model creates difficulties for obtaining direct solutions so numerical methods become necessary. The research applies Hermite polynomial collocation with Caputo fractional orders to convert the system into a nonlinear algebraic problem and performs the computations through Maple software. The simulation outcomes prove HCM and LADM match epidemic patterns correctly but HCM delivers better accuracy values and completes runs more swiftly. The research emphasizes the importance of memory effects in fractional-order models which shows their ability to determine SARS-CoV-2 variant transmission dynamics. HCM exhibits exceptional predictive precision which provides essential value to policy-makers who need to establish adaptable public health strategies for new COVID-19 variant control. Supplementing epidemiological models with fractional orders improves prediction accuracy which proves vital for public health official planning of interventions in outbreaks. For further refinement and investigation.

REFERENCES

Abdullah, M., Yaseen, M., & De la Sen, M. (2022). An efficient collocation method based on Hermite formula and cubic B-splines for numerical solution of the Burgers' equation. Mathematics and Computers in Simulation, 197, 166–184. Elsevier.

Adebisi, A. F., Olayiwola, M. O., Adediran, I. A., &Alaje, A. I. (2024). A novel mathematical model and homotopy perturbation method analyzing the effects of saturated incidence and treatment rate on COVID-19 eradication. Iranian Journal of Science, 48(3), 625–636.

Adebisi, A. F., Uwaheren, O. A., Abolarin, O. E., Raji, M. T., Adedeji, J. A., & Peter, O. J. (2021). Solution of typhoid fever model by Adomian decomposition method. Journal of Mathematics and Computer Science, 11(2), 1242–1255.

Adewale Adedokun, K., OyedunsiOlayiwola, M., AdedapoAlaje, I., OlarewajuYunus, A., OlalekanOladapo, A., &Oyeleye Kareem, K. (2024). A Caputo fractional-order model of tuberculosis incorporating enlightenment and therapy using the Laplace–Adomian decomposition method. International Journal of Modelling and Simulation, 1–15. Taylor & Francis.

Aboiyar, T., &Enonche, F. Probabilists' Hermite Collocation Method for solving two point higher order linear boundary problems of ordinary differential equations. [Publisher not specified].

Ahmed, S., Jahan, S., Shah, K., &Abdeljawad, T. (2024). On mathematical modelling of measles disease via collocation approach. AIMS Public Health, 11(2), 628. AIMS Press.

Alaje, A. I., &Olayiwola, M. O. (2023). A fractional-order mathematical model for examining the spatiotemporal spread of COVID-19 in the presence of vaccine distribution. Healthcare Analytics, 4, 100230. https://doi.org/10.1016/j.health.2023.100230. Elsevier.

Anietie, E. U., &Ini-Obong, E. (2022). SEIR model with a vaccination parameter using COVID-19 as a case study. The Journals of the Nigerian Association of Mathematical Physics, 63, 135–142.

Apostolopoulos, V., Feehan, J., &Chavda, V. P. (2024). How do we change our approach to COVID with the changing face of disease? Expert Review of Anti-infective Therapy, 22(5), 279–287. Taylor & Francis.

Asimiyu, O. O., Yunus, A. O., Omoloye, M. A., &Olayiwola, M. O. (2025). Novel approaches to malaria control and eradication using fractional-order modeling and numerical simulations. Next Research, 100205.

Aydin, S. (2018). The foundational SIR model: Dividing the population into susceptible, infected, and recovered compartments. Journal of Epidemiological Studies, 10(2), 45–60.

Erdem, K., &Yalçınbaş, S. (2012). Bernoulli polynomial approach to high-order linear differential-difference equations. AIP Conference Proceedings, 1479, 360–364. https://doi.org/10.1063/1.4756138

Gheisari, F. (2024). Navigating the future of COVID-19 outbreaks: Trends, challenges, and strategies in 2024. Journal of Clinical Case Studies, Reviews & Reports, 2(3), 1–16.

Gülsu, M., Yalman, H., Öztürk, Y., &Sezer, M. (2011). A new Hermite Collocation Method for solving differential-difference equations. Applied and Applied Mathematics, 6, 1856–1869.

Henka, Y., Lemita, S., &Aissaoui, M. Z. (2023). Hermite wavelets collocation method for solving a Fredholmintegro-differential equation with fractional Caputo–Fabrizio derivative. Proyecciones (Antofagasta), 42(4), 917–930.

Hussain, R., Ali, A., Chaudary, A., Jarral, F., Yasmeen, T., &Chaudary, F. (2017). Numerical solution for mathematical model of Ebola virus. International Journal of Advanced Research, 5, 1532–1538.

Jacob, E., Olumi, T., Ibrahim, A., & Suberu, I. (2022). Numerical simulation of coronavirus disease epidemic based on established susceptible-exposed-infectious-recovered-undetectable-susceptible model. *Fudma journal of sciences*, *6*(5), 224-230. https://doi.org/10.33003/fjs-2022-0605-1731

Manohara, G., &Kumbinarasaiah, S. (2024). Numerical approximation of fractional SEIR epidemic model of measles and smoking model by using Fibonacci wavelets operational matrix approach. Mathematics and Computers in Simulation, 221, 358–396. Elsevier.

Mbainguesse, D., Seid, A. M., Abbo, B., &Paré, Y. (2024). Hermite operational matrix and collocation methods for solving linear fractional Fredholmintegro-differential equation. Far East Journal of Applied Mathematics, 117(1), 1–18.

Moreno Martín, S., RosGiralt, L., & Celaya Llover, E. (2022). Collocation methods for second order systems. In Proceedings of the XVIII Robotics: Science and Systems Conference (RSS) (pp. 1–11).

Nwokoye, C. H., Mbeledogu, N. N., Paul, R. U., &Ugwunna, C. (2022, October). Complementing malware epidemic agent-based models with routing protocols of communication networks using NetLogo. In International Conference on Information and Communication Technology for Competitive Strategies (pp. 833–847). Springer Nature Singapore.

Olayiwola, M. O., &Alaje, A. I. (2024). Mathematical modelling of diphtheria transmission and vaccine efficacy using Nigeria. Modeling Earth Systems and Environment, 10(3), 3941–3967. Springer.

Olayiwola, M. O., &Yunus, A. O. (2024). Mathematical analysis of a within-host dengue virus dynamics model with adaptive immunity using Caputo fractional-order derivatives. Journal of Umm Al-Qura University for Applied Sciences, 1–20.

Olayiwola, M. O., Alaje, A. I., &Yunus, A. O. (2024a). Modelling the impact of education and memory on the management of diabetes mellitus using Atangana–Baleanu–Caputo fractional order model. Nonlinear Dynamics, 1–21. Springer.

Olayiwola, M. O., Alaje, A. I., &Yunus, A. O. (2024b). A Caputo fractional order financial mathematical model analyzing the impact of an adaptive minimum interest rate and maximum investment demand. Results in Control and Optimization, 14, 100349. Elsevier.

Olayiwola, M. O., Adebisi, A. F., & Abubakre, B. (2025). Mathematical modeling of a nonlinear SEIR model of COVID-19 via the numerical solution of Hermite collocation method. *Nonlinear Science*, 100048.

Pirim, A. N., &Ayaz, F. (2016). A new technique for solving fractional order systems: Hermite Collocation Method. Springer Physics Mathematics and Statistics, 7, 2307. Springer.

Srinivasa, K., Baskonus, H. M., & Guerrero Sánchez, Y. (2021). Numerical solutions of the mathematical models on the digestive system and COVID-19 pandemic by Hermite wavelet technique. Symmetry, 13(12), 2428. MDPI.

Yadav, R. S. (2020). Mathematical modeling and simulation of SIR model for COVID-2019 epidemic outbreak: A case study of India. medRxiv, 2020–05. https://doi.org/10.1101/2020.05.20.20108308

Yunus, A. O., &Olayiwola, M. O. (2024a). The analysis of a novel COVID-19 model with the fractional-order incorporating the impact of the vaccination campaign in

Nigeria via the Laplace–Adomian Decomposition Method. Journal of the Nigerian Society of Physical Sciences, 1830–1830.

Yunus, A. O., &Olayiwola, M. O. (2024b). Mathematical modeling of malaria epidemic dynamics with enlightenment and therapy intervention using the Laplace–Adomian decomposition method and Caputo fractional order. Franklin Open, 100147. Elsevier.

Yunus, A. O., &Olayiwola, M. O. (2025). Dynamics of Ebola virus transmission with vaccination control using Caputo–Fabrizio fractional-order derivative analysis. Modeling Earth Systems and Environment, 11(3), 1–18. Springer.

Yunus, A. O., Olayiwola, M. O., Adedokun, K. A., Adedeji, J. A., &Alaje, I. A. (2022). Mathematical analysis of fractional-order Caputo's derivative of coronavirus disease model via Laplace Adomian decomposition method. Beni-Suef University Journal of Basic and Applied Sciences. https://doi.org/10.1186/s43088-022-00326-9 . Springer.

Yunus, A. O., Olayiwola, M. O., Omoloye, M. A., &Oladapo, A. O. (2023). A fractional order model of Lassa disease using the Laplace–Adomian Decomposition Method. Health Analytics Journal. http://doi.org/10.1016/j.health.2023.10.100167. Elsevier.

Yüzbaşı, Ş., &Yıldırım, G. (2023). A Pell–Lucas collocation approach for an SIR model on the spread of the novel coronavirus (SARS CoV-2) pandemic: The case of Turkey. Mathematics, 11(3), 697. MDPI.